Published OnlineFirst September 28, 2018; DOI: 10.1158/1541-7786.MCR-18-0460

Signal Transduction

Molecular Cancer Research

miR-122-5p Expression and Secretion in Melanoma Cells Is Amplified by the LPAR3 SH3–Binding Domain to Regulate Wnt1

Charnel C. Byrnes, Wei Jia, Ali A. Alshamrani, Sudeepti S. Kuppa, and Mandi M. Murph

Abstract

The lysophosphatidic acid receptor-3 (LPAR3) is a G protein–coupled receptor that mediates viability among malignant cells and aggressiveness among certain tumors. The study's objective was to determine the interplay between LPAR3 and miRNAs to impact key cellular signaling pathways. Using SK-Mel-2 and SK-Mel-5 melanoma cells, wild-type and mutated receptors were stably expressed to explore molecular mechanisms. LPAR3 signaling induced miR-122-5p intracellularly and subsequently its inclusion into exosomes. This amplification resulted in less abundant Wnt1, maintenance of GSK3 inactivation and to a lesser extent, partial degradation of β-catenin. The surge in miR-122-5p and reduction in Wnt1 originated from signaling at the Src homology 3 (SH3) ligand–binding motif within the third intracellular loop of LPAR3, because mutant receptors did not increase miR-122-5p and had a weakened capacity to reduce Wnt1. In addition, a key mediator of melanoma survival signaling, the peroxisome proliferator-activated receptor gamma coactivator 1-α (PPARGC1A/PGC1), was involved in miR-122-5p transcription. In conclusion, this study highlights the powerful role miRNAs have in fine-tuning specific G protein–coupled receptor-mediated signaling events by altering the transcription of signaling transduction pathway components. This study also identifies that LPAR3 increases miR-122-5p expression, which occurs mechanistically through the SH3 domain and helps explain why miR-122-5p increases are detected in cancer patient serum.

Implications: LPAR3 is partially responsible for the production and secretion of miR-122-5p, found in the serum of a wide variety of patients with cancer.

Introduction

The lysophosphatidic acid receptor-3 (LPAR3/Edg-7) is a seven-transmembrane, cell-surface, G-protein–coupled receptor, and the third member of the Endothelial Differentiation Gene (Edg) receptor family, that specifically binds lysophosphatidic acid (1, 2). This receptor is also a major promoter of long-term viability among melanoma cells (3, 4). Besides melanoma, enforced expression of LPAR3 increases malignancy among breast and ovarian cancers *in vivo*. Animals with excess LPAR3 display a shift toward aggressive tumors, including comparatively more metastasis, more ascites, and enhanced cancer signaling pathways (5, 6).

We have previously established that the Src homology 3 (SH3) ligand–binding motif, within the third intracellular loop of the LPAR3 is the critical mechanistic region that facilitates melanoma cell viability. This region was mutated by replacing both of the required residues within the recognition motif, valine and proline, to alanines, resulting in a receptor called the 2aa-mutant, which reduces calcium signaling and abolishes ERK/MAPK activity (3). Thus, the region plays a major role in mediating LPAR3 signaling.

To understand the impact of signaling pathways beyond receptor activation and subsequent protein phosphorylation, it is now becoming more apparent that miRNAs play a significant regulatory role. miRNAs are single-stranded RNA sequences approximately 22 nucleotides in length that modulate gene expression. Although miRNAs do not code for genes, these molecules regulate genes at the posttranscriptional level through fine-tuning adjustments in mRNA expression by acting as mRNA corepressors or coactivators (7). Therefore, the presence or absence of miRNA expression can significantly alter events within a signaling pathway.

Equally important to the miRNA expression profiles is the export of miRNA out of the cell. One method for miRNA secretion from the cell is via exosomes, 30–100 nm vesicles that are released when multivesicular endosomes fuse with the plasma membrane (8, 9). Exosomes can also contain DNA, RNA, proteins, lipids, and enzymes that metabolize lipids (10–12). Exosome secretion appears to be a signature of tumor cell aggressiveness, which serves as communication with the microenvironment to precondition tissue and facilitate tumorigenesis (13–18). Speculation exists that the signaling of "certain...but not all" G protein–coupled receptors are the fundamental contributors of exosome secretion (19).

Department of Pharmaceutical and Biomedical Sciences, The University of Georgia, Athens, Georgia.

Note: Supplementary data for this article are available at Molecular Cancer Research Online (http://mcr.aacrjournals.org/).

Corresponding Author: Mandi M. Murph, The University of Georgia, 240 W Green Street, Athens, GA 30602. Phone: 706-583-0216; Fax: 706-542-7378; E-mail: mmurph@uga.edu

doi: 10.1158/1541-7786.MCR-18-0460

Published OnlineFirst September 28, 2018; DOI: 10.1158/1541-7786.MCR-18-0460

The miRNA of interest in this study is miR-122-5p. It is widely expressed in tissue, but is most prominently implemented in hepatocellular carcinoma (HCC) etiology and is expressed at an abundant level in liver. However, serum from patients with cancer shows an increase of miR-122-5p across a broad range of tumor types (Supplementary Fig. S1), suggesting a far more widespread distribution than what might be appreciated. Similarly, a study defining miRNAs in the serum of patients with melanoma showed a high level of miR-122-5p (20). Although miRNA expression is generally tissue specific, miR-122-5p suppresses the expression of the Wnt-1 protein in glioma and HCC cells (21, 22), again suggesting impacts on multiple systems.

Developmental studies investigating signaling mechanisms that used LPAR3 morpholino oligonucleotides determined that Wnt signaling is a critical pathway mediated by this receptor (23). In a normal cell, the canonical Wnt/β-catenin signaling pathway serves to regulate β-catenin proteolysis, whereby phosphorylated β-catenin is degraded and unphosphorylated protein translocates to the nucleus to function as a transcriptional coactivator. Unregulated β-catenin promotes tumorigenesis by accumulating in the nucleus and incessantly stimulates transcription of Wnt target genes (24). In addition, exogenous expression of the LPAR3 induces phosphorylation and inactivation of glycogen synthase kinase 3 (GSK-3) and activation of PI3K (25).

Herein, we sought to determine how LPAR3 fine-tunes the expression of specific miRNA as part of its shift to malignant cellular signaling, and if so, which miRNA(s) and mechanistic components are involved. Data showed that abundant miR-122-5p was expressed as a result of LPAR3 expression/activation and a pool of miR-122-5p was also secreted from the cell in exosomes. As a result of the third intracellular loop of LPAR3 that amplifies miR-122-5p, signaling pathways are altered; for example, GSK-3β phosphorylation and Wnt-1 abundance are modified. To our knowledge, no studies have previously reported the relationship between miR-122-5p and the lysophosphatidic signaling pathway, nor that mechanistically, LPAR3 is utilized to regulate these events.

Materials and Methods

Materials

The human cancer cell lines SK-Mel-2 and SK-Mel-5 were purchased from the NCI (Frederick, MD). HepG2 human liver cancer cells were purchased from Sigma-Aldrich. COS-7 African green monkey kidney cells were purchased from ATCC. Cells were maintained in RPMI or DMEM (Mediatech) supplemented with 10% FBS (Atlanta Biologicals) at 37°C in a humidified atmosphere of 5% CO_2. Generation of LPAR3-stable cell lines was performed as described previously (3). (2S)-3-[(hydroxymercaptophosphinyl)oxy]-2-methoxypropyl ester (OMPT) was purchased from Cayman Chemicals and regularly dissolved in DMSO (Corning).

miRNome screening

SK-Mel-2 parental, wild-type, and mutant cell lines were grown in culture prior to the extraction of small RNA using the mirVANA kit (Ambion). Whole-genome screening for miRNAs was performed as described previously (26). The data were analyzed to find miRNAs differentially expressed between wild-type and mutant cell lines, which were assessed in comparison with parental.

Human serum miR-122-5p levels

Publicly available data were downloaded from the NCBI's Gene Expression Omnibus (GEO) Datasets (https://www.ncbi.nlm.nih.gov/gds) and mined for miR-122-5p. Results from GSE106817 ($n = 4{,}004$) are shown as a bar graph of the average units.

qRT-PCR

Total RNA was isolated from tissues or cells using TRIzol reagent (Thermo Fisher Scientific) followed by reverse transcription for cDNA synthesis from mRNA or miRNA using iScript cDNA Synthesis Kit (Bio-Rad) and TaqMan MicroRNA Reverse Transcription Kit (Thermo Fisher Scientific), respectively. Detection of miR-122-5p was performed using primers from TaqMan MicroRNA Assays Kit (Thermo Fisher Scientific). Only the mature miR-122-5p sequence was provided as 5′-UGGAGUGUGACAAUGGUGUUUG-3′. Most of the primers used were based on sequences generated by Primer Bank's algorithm (http://pga.mgh.harvard.edu/primerbank/). More specifically, the data presented used:

β2-microglobulin primers (5′-GTGGCCTTAGCTGTGCTCG-3′ forward and 5′-ACCTGAATGCTGGATAGCCTC-3′ reverse); cyclin G1 (CCNG1) primers (5′-GAGTCTGCACACGATAATGGC-3′ forward and 5′-GTGCTTGGGCTGTACCTTCA-3′ reverse); dual specificity protein phosphatase 4 (DUSP4) primers (5′-GGCGGCTATGAGAGGTTTTCC-3′ forward and 5′-TGGTCGTGTAGTGGGGTCC-3′ reverse); fibronectin-1 primers (5′-CGGTGGCTGTCAGTCAAAG-3′ forward and 5′-AAACCTCGGCTTCCTCCATAA-3′ reverse); GAPDH primers (5′-GGAGCGAGATCCCTCCAAAAT-3′ forward, 5′-GGCTGTTGTCATACTTCTCATGG-3′ reverse); lysyl oxidase (LOX) primers (5′-CCAGGGCACAGCAGACTTC-3′ forward and 5′-GTAGTGGCTGAACTCGTCCA-3′ reverse); PGC-1α primers (5′-TCTGAGTCTGTATGGAGTGACAT-3′ forward, 5′-CCAAGTCGTTCACATCTAGTTCA-3′ reverse); and 18s rRNA primers (5′-AGAAACGGCTACCACATCCA-3′ forward, 5′-CCCTCCAATGGATCCTCGTT-3′ reverse). Samples were generally run in sextuplicates and the data are presented as bar graphs displaying the averages of results and mean SD from a representative experiment that was repeated at a minimum of three times.

Extracellular miRNA levels were assessed using the miRCURY Exosome Isolation Kit and miRCURY RNA Isolation Kit (Exiqon) to isolate exosomes from cell culture media and the following total RNA extraction from the exosomes, respectively. The subsequent reverse transcription and RT-PCR for intracellular and extracellular miRNA was performed using TaqMan MicroRNA Reverse Transcription Kit, TaqMan Universal PCR Master Mix and primer sets in TaqMan MicroRNA Assays Kit (Thermo Fisher Scientific).

Microfluidics quantification of exosomes

Exosomes from 72-hour conditioned medium secreted from cell cultures were extracted. All conditions were compared with each other, using the parental cells as a baseline. A NanoSight (Malvern) was used to measure the concentration of particles sized 30–100 nm per mL of fluid and generate data derived from particle size, measurements of the peaks, and total concentration of all particles detected up to 500 nm in size. Representative data that were repeated are shown. The Malvern software automatically

Published OnlineFirst September 28, 2018; DOI: 10.1158/1541-7786.MCR-18-0460

generated time-lapsed images as well as heatmaps that depict exosomal secretion and presence of multivesicular bodies.

Immunoblotting and protein analysis

Cells were seeded in 6-well plates at a density of 2.25–4.5 $\times$ 10^5 cells per well. Cells were transfected after 24 hours of incubation following the protocol provided by the manufacturer. Mock cells were transfected with Dharmafect reagent only (Dharmacon), and another group was transfected with 50 nmol/L miR-122-5p mimic in the 2aa-mutant cell line. Whole-cell lysates were collected after 24 hours and protein concentrations were determined using the Pierce BCA Protein Assay Kit (Thermo Fisher Scientific) to obtain 20 mg of loading sample. Protein samples were resolved on 4% stacking and 12% resolving gels. Proteins were subsequently transferred onto nitrocellulose membranes, which were blocked with 5% milk overnight. Membranes were then exposed to 1:1,000 primary antibodies from Cell Signaling Technology, including the β-Catenin Sampler Kit (#295), with total β-catenin, phospho-β-catenin (Ser675), (Ser552), and (Ser33/37/Thr41), the GSK-3 Antibody Sampler Kit (#9369) with total and phospho-GSK3α and GSK-3β (Ser9 and Ser21), Axin1 (#2087), Dvl2 (#3224), phospho-LRP6 (Ser1490; #2568), and LRP6 (#3395). Following TBST washes, blots were exposed to 1:2,000 anti-rabbit secondary antibody (Cell Signaling Technology). Representative blots are shown from repeated experiments that yielded similar results. The NIH's ImageJ software was used to quantify protein band intensities, which were normalized to parental cells as well as GAPDH. In other experiments, the levels of GSK-3 were assessed by the Reverse Phase Protein Array Core facility (The University of Texas MD Anderson Cancer Center, Houston, TX) as described previously (27, 28). The results are presented as mean averages ±SEM in bar graphs for comparison.

Immunofluorescence and quantification

To detect Wnt-1, cells were plated in 96-well plates at a density of 3,000 cells per well. Following an incubation for 24 hours to allow adherence, cells were fixed with 2% formaldehyde for 10 minutes. Subsequently, ice-cold methanol was added to permeabilize the cells for 60 seconds. The anti-Wnt1 antibody #ab15251 (Abcam) was added at a dilution of 1:200 and incubated for 1 hour. Following PBS washes, the secondary antibody was added with 10% saponin, washed, and sealed. The plates were scanned using the Cellomics ArrayScan VTI (Thermo Fisher Scientific) high content imaging platform, to automatically measure and collect data including intensity, cell count, and morphology. Over 250 cells were assessed per experiment that was repeated four times.

To detect perinuclear and nuclear β-catenin proteins, cells were plated in 96-well plates at a density of 5,000 cells per well. Following 48-hour incubation for adherence, cells were fixed with 2% formaldehyde for 10 minutes. Cells were washed three times with PBS followed by permeabilization with ice-cold methanol for 3 minutes. Following three subsequent washes with PBS, cells were blocked overnight in 10:1 PBS/FBS. Cells were then exposed to 1:100 total-β-catenin (Cell Signaling Technology) primary antibody with 10% saponin for 1 hour. Following three washes with PBS/FBS, 1:500 anti-rabbit IgG Fab2 Alexa Fluor 488 secondary antibody (Cell Signaling Technology) was added with 10% saponin, incubated for 1 hour, washed, and sealed. The plates were scanned using the, Cellomics ArrayScan VTI, which automatically measures and collects data including intensity, colocalization, cell count, and morphology (Thermo Fisher Scientific). More specifically, the ring and object intensity algorithms assessed both total and average perinuclear intensity as well as both total and average nuclear intensity of Alexa Fluor 488, respectively. Between 500 and 1,000 cells were measured for data collection in >25 different fields. After data analysis was completed, three representative images were selected and identical contrast enhancements were performed to enhance the visualization of the antibody by minimizing the background as presented here.

Stable LPAR3 expression in HepG2

The human Edg-7/LPA_3 receptor was overexpressed in HepG2 cells using pcDNA3.1 and an expression plasmid for LPAR3 with an HA epitope tag for identification, using a method described previously (3). Messenger RNA was extracted, reversely transcribed into cDNA, and analyzed with qPCR using the same protocols and primers for LPA1-6 as stated previously. The Bioanalyzer PCR products were evaluated by the Bioanalyzer 2100 (Agilent Technologies) using the method described previously (4). Each PCR sample was individually analyzed on the Agilent DNA 1000 chip in gel-dye matrix for 35 minutes and the resultant gel image is shown.

Transient transfections

Cells were plated at a density of 2.5 $\times$ 10^5 cells per well into 6-well plates. Cells were transfected with either 50 nmol/L miR-122-5p mimic, 50 nmol/L siPGC-1α, 50 nmol/L miR-122-5p antagomir, or siControl using Dharmafect reagent (Dharmacon). Dharmafect reagent alone was also used as a secondary control group. Transfections were allowed to proceed for 72 hours, with a media change using DMEM containing 10% FBS (complete medium) after 24–36 hours. A partial knockdown of the LPAR3 (50 nmol/L siLPAR3 = 73% expression) was performed to

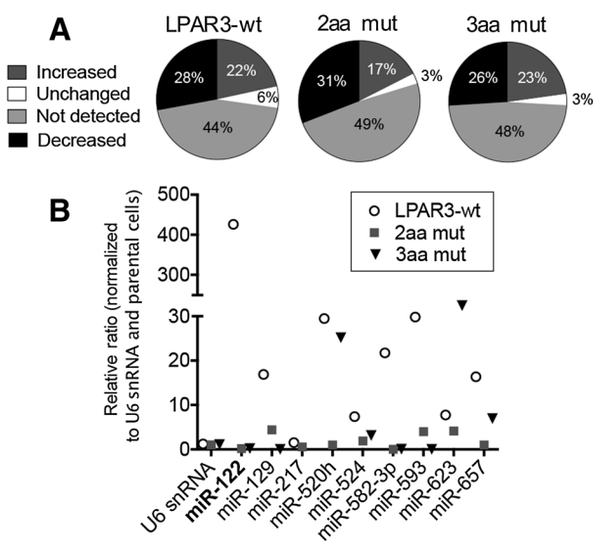

Figure 1.

Expression of LPAR3 increases miR-122-5p. SK-Mel-2 parental, wild-type, and mutant receptor–expressing cells had small RNAs extracted prior to performing miRNA screening using TaqMan arrays. **A,** Compared with parental cells, LPAR3-wt cells had an increase in 22% of the miRNAs on the array and 6% were unchanged. Cells expressing mutant LPAR3 were similar in nature. **B,** Randomly chosen miRNAs detected on the array are displayed as a comparison with the results obtained from miR-122-5p.

Published OnlineFirst September 28, 2018; DOI: 10.1158/1541-7786.MCR-18-0460

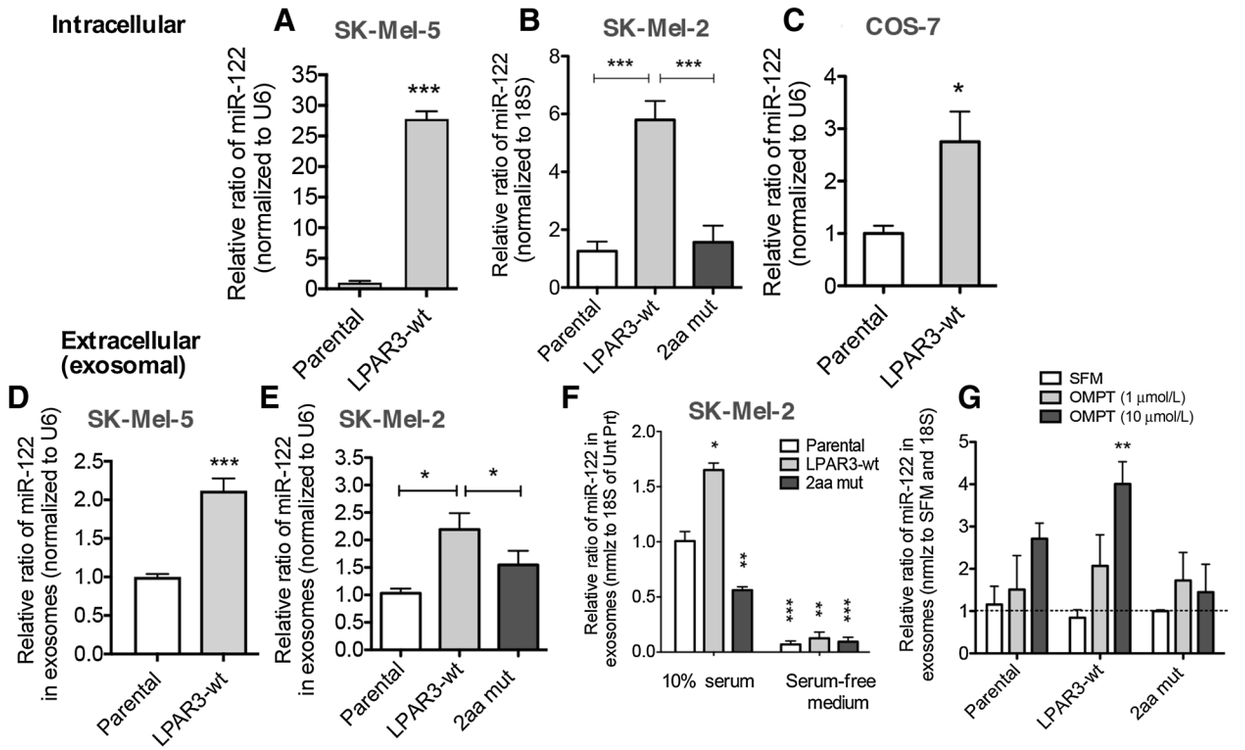

Figure 2.

Functional LPAR3 enhances extracellular secretion of miR-122-5p. Intracellular miR-122-5p was measured using relative qRT-PCR in three stable cell lines, SK-Mel-5 (**A**), SK-Mel-2 (**B**), and COS-7 (**C**), all with enforced expression of wild-type LPAR3 or a mutant, 2aa-mut, with two residues substituted in the third intracellular loop. Exosomes were isolated in the conditioned medium of SK-Mel-5 (**D**) and SK-Mel-2 cells (**E**) and assessed for the presence or absence of miR-122-5p, relative to parental control and normalized to U6. SK-Mel-2 cells were either serum-starved (**F**) or treated with OMPT (**G**), an LPAR3 agonist, prior to exosome isolation and analysis of miR-122-5p.

maintain cell viability (4). In certain experiments, cells were exposed to a final concentration of 1 μmol/L OMPT overnight. Cells were harvested using TRIzol reagent.

Functional assays

For migration, SK-Mel-2 cells (parental, LPAR3-wt, and 2aa-mut) were plated in 24-well plates with 1×10^5 cells. After 24 hours of incubation at 37°C, cells were transfected using DHARMAfect with 50 nmol/L siControl (siCON), siLPAR2, siPGC1α, or miR-122 mimic. Cells were serum-starved the following day and after another 24 hours of incubation, all cells were exposed to 1 μmol/L OMPT for 24 hours. Cells were trypsinized and 1×10^5 cells were added to transwell inserts and left to grow for 48 hours. Transwells were then exposed to 1 mL of 0.5% Crystal Violet in 30% methanol. After 3×5 minute washes with $1\times$ PBS, cells inside the transwells were removed with sterilized cotton swabs to assess only the cells that migrated through the 8-μm pores. Stained cells were imaged with microscopy, and counted using ImageJ. Proliferation and viability assays were performed as described previously (3, 26).

Tissue assessment for miRNA-122

Kidney ($n = 3,3$), heart ($n = 6,12$), liver ($n = 6,10$), and lung ($n = 2,10$) tissues of wild-type mice and LPAR3-knockout mice, respectively, were kindly provided by Dr. Xiaoqin Ye at The University of Georgia (Athens, GA). Total RNA was isolated from the tissues using TRIzol reagent (Thermo Fisher Scientific) followed by reverse transcription for cDNA synthesis from mRNA or miRNA using iScript cDNA Synthesis Kit (Bio-Rad) and TaqMan MicroRNA Reverse Transcription Kit (Thermo Fisher Scientific), respectively. The primers for LPAR3 are 5′- TGACAAGCGCATGGACTTTTTC - 3′ (forward) and 5′-AGTGGAACTTCCGGTTTGTG - 3′ (reverse).

Statistical analysis

The data were evaluated by statistical tests and comparing the means between three or more groups using ANOVA. Subsequent post tests to determine the significance relied on the Bonferroni's multiple comparison. If there were comparisons between two groups, Wilcoxon–Mann–Whitney test or the Student t test was used. *, $P < 0.05$; **, $P < 0.01$ and ***, $P < 0.001$ indicate the levels of significance. Both GraphPad Prism and Microsoft Excel were used to perform these calculations.

Results

LPAR3 amplifies miR-122-5p expression and subsequent exosomal secretion through its SH3 domain

To understand whether and how the LPAR3 specifically exploits miRNA to impact key cellular signaling pathways in melanoma, we commenced a candidate screen approach. Because of

Published OnlineFirst September 28, 2018; DOI: 10.1158/1541-7786.MCR-18-0460

negligible LPAR3 expression in SK-Mel-2 cells (3), we overexpressed wild-type or mutant LPAR3s and screened with TaqMan Arrays to identify a miRNA amplified among LPAR3-wt cells, but not 2aa- or 3aa-mut cells (Fig. 1A). Thus, the results revealed miR-122-5p (Fig. 1B).

To verify these results, the relative amount of intracellular miR-122-5p was measured among SK-Mel-5 (Fig. 2A), SK-Mel-2 (Fig. 2B), and COS-7 cells (Fig. 2C). miR-122-5p abundance is dependent on receptor signaling through the SH3 domain because the modified LPAR3 receptor, 2aa-mut, with alanine substitutions in both recognition motif residues, valine and proline, did not show miR-122-5p amplification (Fig. 2B). It should also be noted that the 2aa-mut receptor's expression is comparatively higher than wild-type (Supplementary Fig. S2).

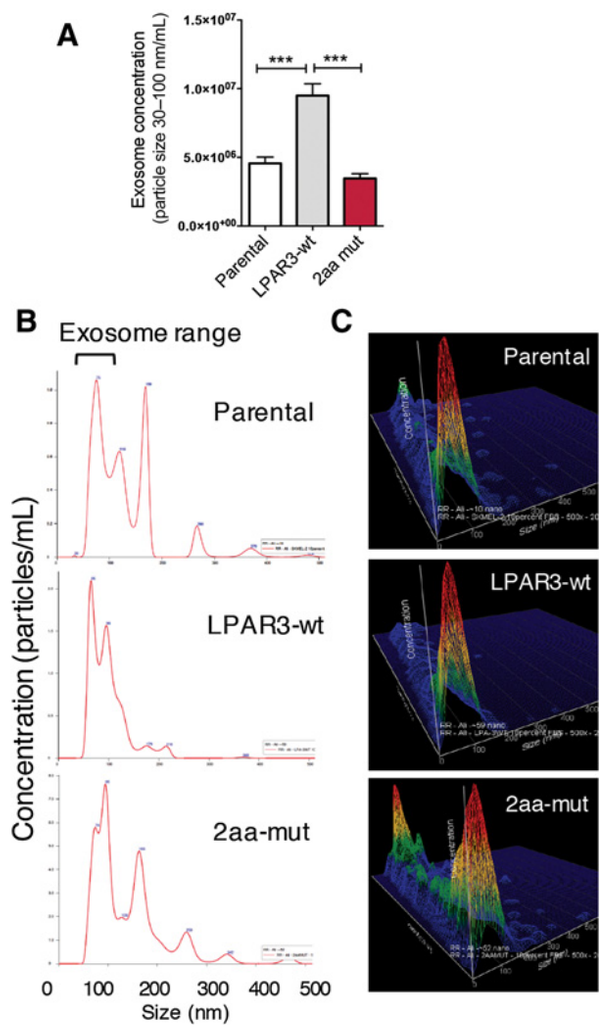

Figure 3.

Exosome production is enhanced by functional LPAR3 expression. Exosomes from 72-hour conditioned medium of SK-Mel-2 cells (parental), versus SK-Mel-2 cells with enforced expression of the LPAR3 (LPAR3-wt) or mutations in the third intracellular loop (2aa-mut) were extracted. The NanoSight (Malvern) measured the concentration of particles sized 30–100 nm per mL (**A**) and the peaks were automatically generated, displaying the concentration of all particles detected through 500 nm (**B**). **C,** Heatmaps show the specific secretion of exosomes exemplified by one strong peak between 30–100 nm in LPAR3-wt cells, versus the 2aa-mut, which has multiple peaks. These results show the LPAR3-wt cells secrete more exosomes by comparison. ***, $P < 0.001$.

Table 1. LPAR3 produces particles within the exosome range

	Parental	LPAR3-wt	2aa-mut
Total particle conc/mL	7.70E + 08	1.07E + 09	6.02E + 08
% of Exosomes (0–150 nm)	70.20%	91.70%	61.60%
% of Exosomes (30–100 nm)	42.70%	63.90%	41.40%
Average particle size (nm)	126.6	98.9	140.2

To assess whether miR-122-5p was exported as a consequence of LPAR3 signaling, we isolated exosomes from conditioned medium and measured miR-122-5p. Exosomes show enriched levels of miR-122-5p in SK-Mel-5 (Fig. 2D) and SK-Mel-2 cells (Fig. 2E). The secretion of miR-122-5p–containing exosomes was significantly inhibited by serum-starving the cells in serum-free medium (Fig. 2F). In contrast, cells overcame the inhibition, when stimulated with 1-oleoyl-2-methyl-sn-glycero-3-phosphothionate (OMPT), a nondegradable, mimic of lysophosphatidic acid and more importantly, an LPAR3-selective agonist (29), with only serum-free medium (Fig. 2G). This suggests a reliance on the stimulation of a functional LPAR3 to elicit an exosome-mediated secretion of miR-122-5p.

We next measured exosomes using dynamic fluidics and observed that SK-Mel-2 cells stably expressing the LPAR3-wt secreted more exosome-sized particles, between 30 and 100 nm, than either the parental SK-Mel-2 or the LPAR3-mutant SK-Mel-2 cells, 2aa-mut (Fig. 3A, ***, $P < 0.001$). Interestingly, the average particle size (nm) became considerably smaller and more uniform among LPAR3-wt cells, in comparison with parental and 2aa-mut cells (Table 1), which also secrete microvesicles between 300 and 500 nm (Fig. 3B). Heatmaps of particle size (Fig. 3C) and time-lapsed images (Supplementary Fig. S3) confirmed this observation. Movies depicting larger particles in solution appear as bright punctate structures, whereas exosomes are hardly discernable.

The LPAR3-miR-122-5p axis affects Wnt-1 abundance

We next assessed whether LPAR3-wt SK-Mel-2 melanoma cells would suppress *WNT1*. If so, we would expect more Wnt-1 protein in the 2aa-mutant cells, due to the fact that they produce less miR-122-5p to inhibit *WNT1* (Fig. 4A). Indeed, more Wnt-1 is present in 2aa-mutant cells (Fig. 4B).

Wnt-1 inactivates GSK-3 after ligands bind to Frizzled receptors, then activate Dishevelled, and subsequent proteins phosphorylate GSK-3β at inactivating Ser9. Notably, the inhibitory Ser9 phosphorylation on GSK-3β surged among 2aa-mutant cells (Fig. 4C and D). Similarly, the 2aa-mutant cells augmented the abundance of Axin1, phosphorylated LDL Receptor Related Protein 6 (pLRP Ser1490), and Dishevelled 2, which inhibit GSK-3β (Fig. 4E). These results were independently corroborated using reverse-phase protein lysate arrays (Fig. 4F).

To corroborate the interplay between the LPAR3 and Wnt-1 abundance, a partial silencing experiment was performed due to widespread cell death after complete LPAR3 knockdown (4). We observed that partial silencing of wild-type LPAR3s or LPAR3-2aa-muts reverses their previous trends in regulating Wnt-1 abundance (Fig. 4G). Taken together, the data suggest that a regulatory Wnt signaling feedback loop stems from the third intracellular loop of the LPAR3 that also regulates viability (3).

Published OnlineFirst September 28, 2018; DOI: 10.1158/1541-7786.MCR-18-0460

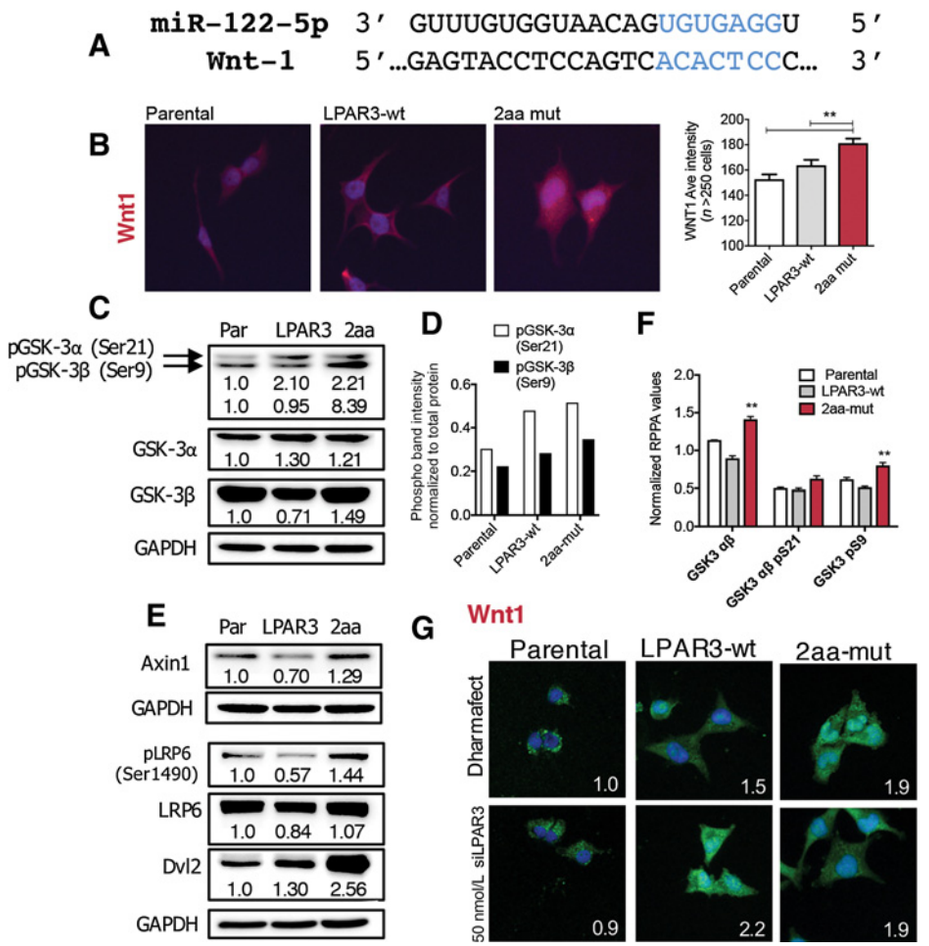

Figure 4.

A lack of miR-122-5p in LPAR3-2aa-mut–expressing cells results in Wnt-1 abundance and inactive phosphorylation of GSK-3β at Serine 9. **A,** Schematic of the miRNA and its known interaction with *WNT1*. **B,** Immunofluorescence and quantification of images of Wnt-1 ($n > 250$) displays an abundance of protein among mutant LPAR3 SK-Mel-2 cells. ***, $P < 0.001$, total Wnt-1 intensity in 2aa-mut. **C,** Immunoblotting of SK-Mel-2 cells demonstrates differences in the abundance of GSK-3α and GSK-3β proteins, as well as the levels of phosphorylation. **D,** Protein band intensities for pGSK-3α(Ser21) and -3β (Ser9) were normalized to total levels of GSK-3, respectively. **E,** Changes in the protein levels of Axin1, LDL Receptor Related Protein 6, and Dishevelled 2 were observed. **F,** Reverse-phase protein array independently confirmed the results of GSK-3 among the three types of SK-Mel-2 cells. **G,** Partial receptor silencing increases Wnt-1 in LPAR3-wt cells. Cells were transfected using exogenous siLPAR3 at concentrations below lethality prior to detection of Wnt-1. Partial silencing reverses the suppression on Wnt-1 mediated by the LPAR3.

PGC-1α is an intermediate in miR-122-5p secretion into exosomes

We sought to bridge the novel link between LPAR3 signaling activation and expression of miR-122-5p by identifying a transcriptional element involved in the mechanism. LPAR3-wt SK-Mel-2 cells display a significant enhancement of *PGC-1α* in comparison with parental and 2aa-mut cells (Fig. 5A, ***, $P < 0.001$). Moreover, the abundance of *PGC-1α* could be heightened further by stimulating the LPA3 receptor with the selective agonist, OMPT (Fig. 5B). The same trend was observed in SK-Mel-5 cells with stable receptor expression (Fig. 5C, ***, $P < 0.001$). Using an siRNA approach to knockdown PGC-1α, we observed a significant inhibition in exosomal miR-122-5p when compared with the control group, transfection with the Dharmafect transfection reagent only (Fig. 5D) with an average knockdown of *PGC-1α* at approximately 50% (Fig. 5E). These data suggest that PGC-1α partially contributes to the mechanism responsible for exosome secretion of miR-122-5p.

To assess the functional contributions of PGC-1α, we next assessed migration, proliferation, and viability of the cells using siRNA. The number of cells migrating through a transwell increased slightly with siPGC-1α or miR-122 for LPAR3-wt and 2aa-mutant SK-Mel-2 cells (Fig. 5F and G). Proliferation in response to OMPT (1 μmol/L) was blunted in the presence of siPGC-1α among LPAR3-wt cells (Fig. 5H). Cell viability was also impacted (**, $P < 0.001$) by the presence of siPGC-1α (Fig. 5I). Taken together, this suggests PGC-1α has partial involvement in mediating the effects of the LPAR3.

β-catenin(Ser33/37/Thr41) phosphorylation is enhanced by miR-122-5p

Because Wnt-1 abundance and GSK-3β phosphorylation are affected by LPAR3, it was necessary to also assess β-catenin signaling. To some extent, total β-catenin protein is diminished by the presence of LPAR3 (Fig. 6A). Similarly, the Akt- and PKA-induced β-catenin phosphorylation sites at Ser675 and Ser552 are nearly absent in 2aa-mut cells and incompletely restored by miR-122-5p. In addition, phosphorylation of β-catenin at Ser33/37/Thr41 is enhanced with exogenous miR-122-5p mimic, suggesting proteasomal degradation is elicited (30). The reverse experiment using the antagomir is unfeasible because it actually increases miR-122-5p (Supplementary Fig. S4).

Correspondingly, β-catenin in parental cells is largely and seemingly located along the adherens junctions between cells (Fig. 6B). Without Wnt-1, β-catenin would not likely accumulate in the cytoplasm, where it would be degraded. Among LPAR3-wt cells, the amount of nuclear localization of total β-catenin is increased and the perinuclear abundance is decreased, in comparison with parental and 2aa-mutant cells

Published OnlineFirst September 28, 2018; DOI: 10.1158/1541-7786.MCR-18-0460

(Fig. 6C; *, $P < 0.05$ and ***, $P < 0.001$, respectively). This is consistent with proteasomal degradation.

miR-122-5p is diminished in heart tissue of LPAR3 knockout mice

In cell types where LPAR3 signaling is important for normal signaling, those tissues should contain less miR-122-5p. Therefore, we procured tissues from knock-out mice missing the first exon of the LPAR3 and measured miR-122-5p. Among heart tissue specimens where LPAR3 plays a dominant role, hardly any miR-122-5p was detected in the LPAR3 knockout mice. However, other tissues with lesser or unappreciated signaling by LPAR3 were unaffected (Supplementary Fig. S5).

Discussion

Herein our results describe a molecular mechanism and signaling pathway that begins with the activation of the cell

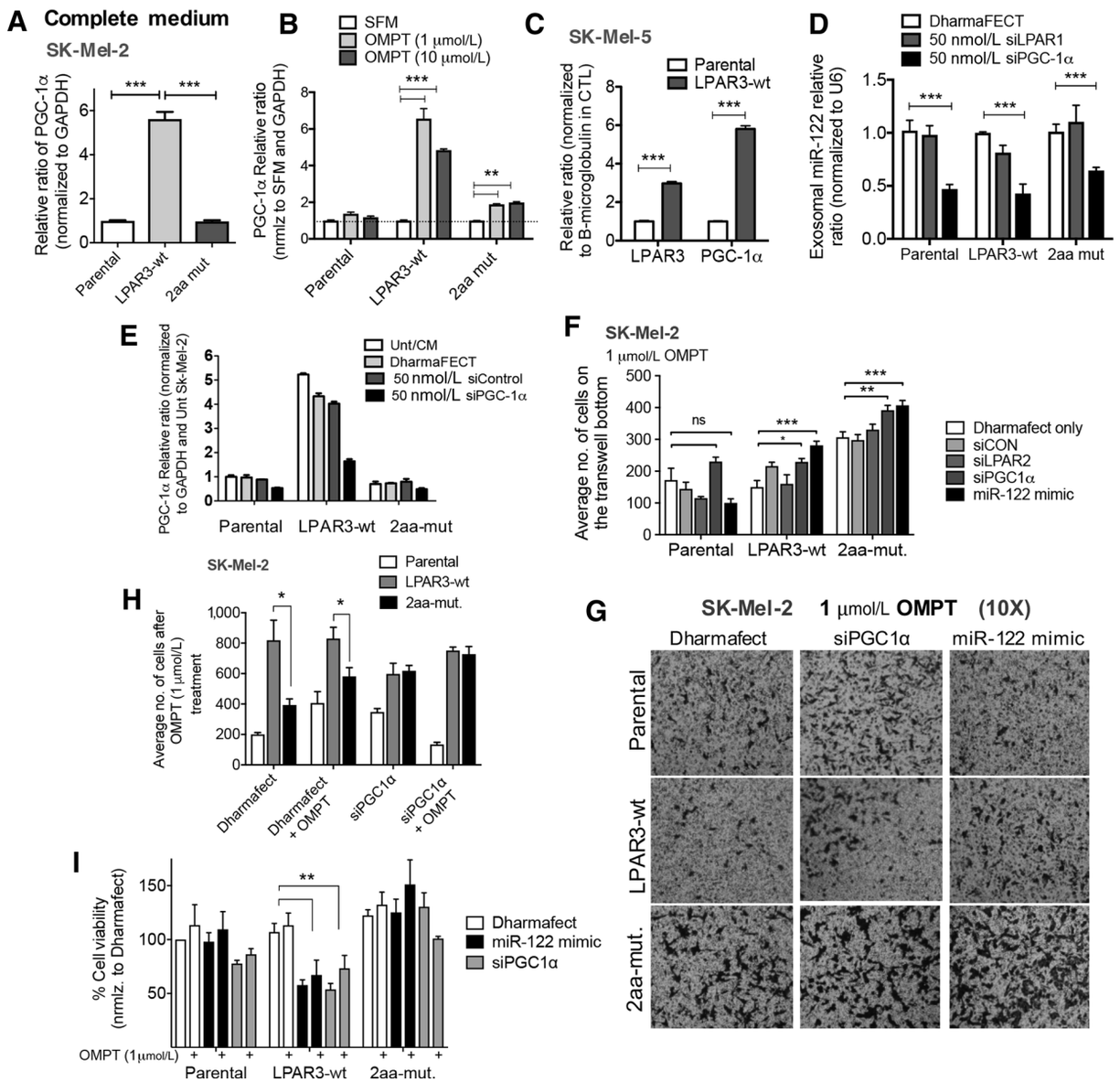

Figure 5.

LPAR3 signaling activation increases PGC-1α expression, which partially regulates miR-122-5p secretion. **A,** The relative ratio of PGC-1α was assessed between SK-Mel-2 cells. ***, $P < 0.001$, LPAR3-wt versus other cells. **B,** Cells were grown under serum-free conditions with and without OMPT prior to assessment for PGC-1α levels. **C,** SK-Mel-5 cells were also assessed for LPAR3 and PGC-1α mRNA expression. **D,** PGC-1α siRNA was used to reduce the expression in SK-Mel-2 cells prior to miR-122-5p extracellular exosome measurement. **E,** Cells were transfected to determine the relative amount of PGC-1α that could be reduced using siRNA, which was approximately 50%. **F,** Migration effects were compared using the average number of cells that migrated through the transwell after treatment with 1 μmol/L OMPT. **G,** Representative images from the bottom of the transwell are shown. **H,** Proliferation was assessed by measuring the number of cells after treatments with OMPT. **I,** Viability was measured after siRNA or miRNA transfection and treatment.

Published OnlineFirst September 28, 2018; DOI: 10.1158/1541-7786.MCR-18-0460

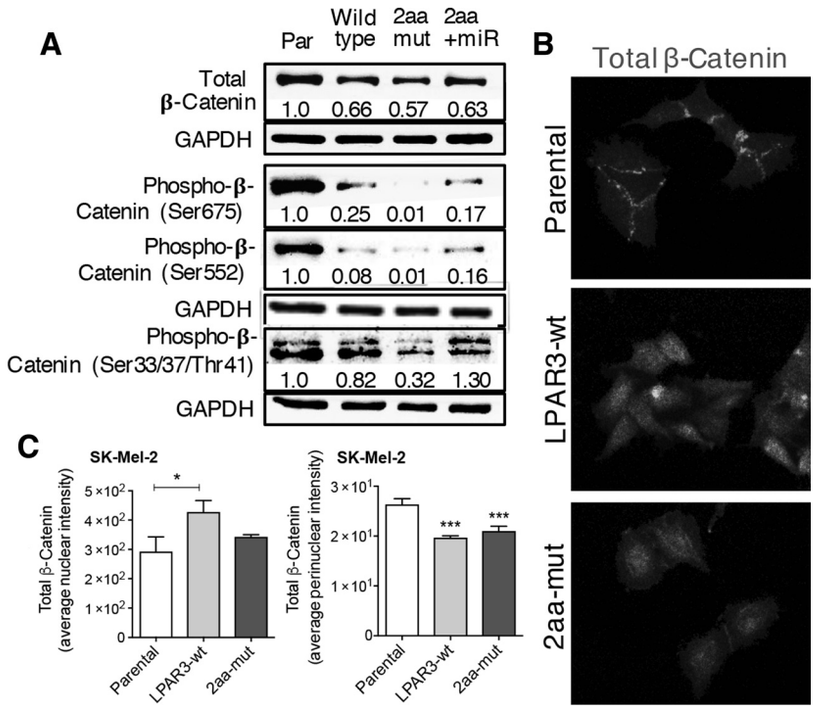

Figure 6.
Degradative phosphorylation site on β-catenin (Ser33/37/Thr41) is enhanced by miR-122-5p. **A,** Immunoblotting for total and phosphorylated β-catenin (Ser675, Ser552, and Ser33/37/Thr41) revealed a decrease in expression among cells expressing either functional or mutant LPAR3, 2aa-mut. Exogenously added miR-122-5p mimic increased Ser33/37/Thr41 phosphorylation. **B,** Localization of β-catenin protein displayed differences between the three types of SK-Mel-2 cells. Parental cells showed β-catenin staining in areas between cells, likely adherens junctions, whereas LPAR3-wt cells localized in the cytoplasm and nuclear region, and 2aa-mut cells exhibited a mix of both phenotypes. **C,** Quantification of staining intensity ($n \approx 500$–1,000) demonstrated a perinuclear β-catenin reduction among LPAR3-wt and 2aa-mut cells.

surface receptor, LPAR3, and leads to the exportation of miR-122-5p into exosomes. The signal is initiated within the Src homology 3 domain and activates the transcriptional coactivator, peroxisome proliferator-activated receptor-gamma coactivator (PGC)-1α, which is partially involved in the transcription of miR-122-5p. Subsequently transcribed miR-122-5p inhibits *WNT1* and is secreted into exosomes. As a result of LPAR3 signaling, miR-122-5p is significantly amplified which results in the following: (i) less Wnt-1 is available, (ii) GSK-3β inactivation is maintained, and (iii) β-catenin is partially degraded (Fig. 7). These differences are largely discernable using the 2aa-mutant receptor. An important dynamic of our study is that it mechanistically connects proven observations from several other studies via a G protein–coupled receptor that is widely expressed in tissue, with an established association to malignancy.

There are other unique aspects of our study, in addition to corroborating signaling pathways through an unknown mechanistic receptor association. For example, although PGC-1α is only partially involved in the effect, it has a critical contribution. PGC-1α is known for its role in lipid regulation and energy metabolism (31). In addition, PGC-1α is implicated in signaling axes associated with cancers such as PML/PGC-1α/PPARα, MITF/PGC-1α, and PGC-1α/ERRα, along with the SIRT1/PGC-1α axis, it is present in stress adaptation, and the p53/PGC-1α axis is involved in determining cell fate (32).

miR-122-5p is renowned as a target with pharmacologic potential (33, 34). Currently, the majority of miR-122-5p studies in the literature are in reference to hepatocellular carcinoma and hepatitis C, with only a small subset of research on other diseases. However, the functionality reported in the latter studies is extraordinary, implicating a much broader role for miR-122-5p in signaling events related to lipid metabolism and metastasis (35, 36). For example, other studies concluded that miR-122-5p regulates cyclin G1 expression and affects the stability of p53 (37). Although cyclin G1 is regulated by miR-122-5p in hepatocellular carcinoma cells, we observed a significant increase in the relative expression of cyclin G1 in SK-Mel-2 cells stably expressing LPAR3, likely resultant from inherent differences between these cell types (Supplementary Fig. S2).

Both a novelty and limitation of our study is the utilization of melanoma cell lines. For example, SK-Mel-2 cells are generally not employed in investigations of miR-122-5p, but they are ideal for LPAR3 studies due to the negligible amounts of LPAR3 they possess (3), which allows for genetic engineering of stable receptors. Thus, our study is likely more translatable to melanoma biology, because our results are consistent with findings reported on miR-122-5p in other systems (21, 35–40). Indeed, a study defining miRNAs in the serum of patients with melanoma showed a high level of miR-122-5p (20). This strongly suggests that the molecular biology identified in our study explains these observations.

To control for LPAR3 signaling, our experiments required receptor specificity. Many cell types express LPAR3 (3), which makes null-receptor model selection challenging. However, using a cell line without LPAR3 and stably expressing receptors is an optimal means to dissect mechanistic features of the receptor. In contrast, if we used cell lines to knock out LPAR3 with siRNA, any surviving populations did not accept the siRNA because siLPAR3 obliterates cell viability and causes massive cell death (4). Therefore, we carefully used partial silencing in our study when needed. Furthermore, using "selective" lysophosphatidic acid species ensures that only the LPAR3 is signaling because there are at least nine known receptors that bind lysophosphatidic acid.

Published OnlineFirst September 28, 2018; DOI: 10.1158/1541-7786.MCR-18-0460

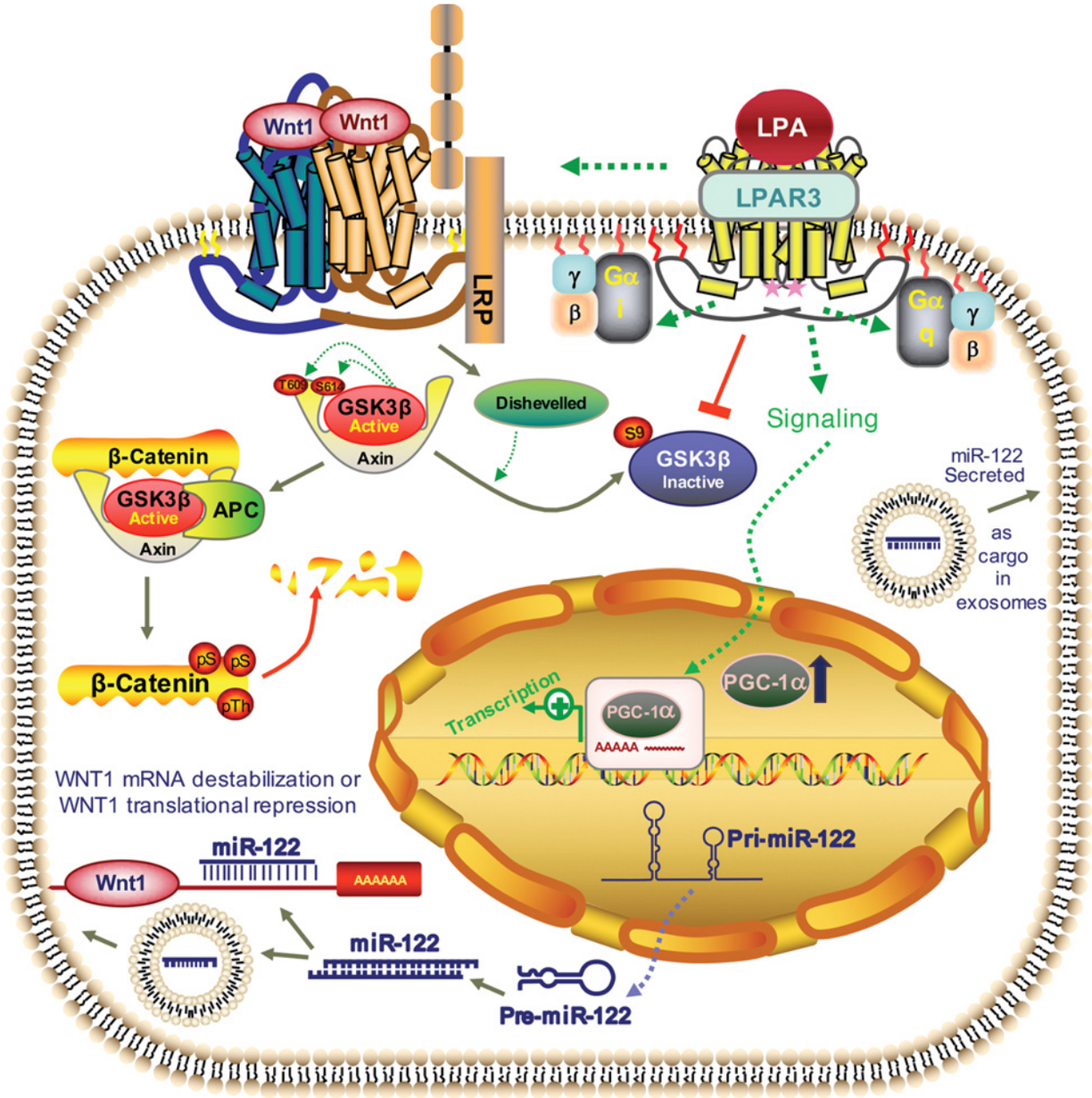

Figure 7.

Schematic representation of LPAR3 signaling with regard to miR-122-5p and Wnt-1 expression. This working model displays the relationship between LPAR3 signaling, β-catenin degradation, PGC-1α transcription, miR-122-5p production, and inhibition of *WNT1*. It also incorporates the exportation of miR-122-5p into extracellular exosomes after repressing *WNT1* mRNA. The pink stars on the LPAR3 dimer depicts the location of the third intracellular loop where the amino acid substitutions were introduced.

A major approach we used to overcome these experimental hurdles (i.e., LPAR3 knock out) was the generation of LPAR3 2aa-mutant. We also coupled this analysis to data generated using tissues from LPAR3 knock-out mice. Previous studies show a complete absence of LPAR1, LPAR2, and LPAR3 expression in liver; rather, the pattern of LPAR3 expression is in heart, lung, kidney, testes, intestines, and developmental brain, which suggests these are key tissues to elucidate receptor function (41).

The power of our study is the novel uncovering of miR-122-5p regulation of, and by, LPAR3 signaling. In addition, the finding that LPAR3 facilitates the exportation of exosomes will impact future melanoma biology studies. This study strongly supports the notions that LPAR3 enhances tumor cell aggressiveness using, at least in part, exosome secretion and that G protein–coupled receptors are fundamental contributors of the same (19). Combined, the tumorigenic role of LPAR3 is upheld with new experimental results that push this idea into new areas.

Published OnlineFirst September 28, 2018; DOI: 10.1158/1541-7786.MCR-18-0460

Future studies will address the mechanism of miR-122-5p exosomal secretion and the impact miR-122-5p signaling has on other study models.

Disclosure of Potential Conflicts of Interest

No potential conflicts of interest were disclosed.

Authors' Contributions

Conception and design: M.M. Murph
Development of methodology: C.C. Byrnes, W. Jia, A.A. Alshamrani, M.M. Murph
Acquisition of data (provided animals, acquired and managed patients, provided facilities, etc.): W. Jia, S.S. Kuppa, M.M. Murph
Analysis and interpretation of data (e.g., statistical analysis, biostatistics, computational analysis): C.C. Byrnes, A.A. Alshamrani, S.S. Kuppa, M.M. Murph
Writing, review, and/or revision of the manuscript: C.C. Byrnes, M.M. Murph
Administrative, technical, or material support (i.e., reporting or organizing data, constructing databases): C.C. Byrnes, A.A. Alshamrani, M.M. Murph
Study supervision: M.M. Murph

Acknowledgments

The research was supported in part by an American Cancer Society Research Scholar Grant (120634-RSG-11-269-01-CDD) and in part by the NCI of the NIH under award number R21CA208736 (both to M.M. Murph). We would like to thank Rong Li and Christian Lee Anderson for assistance with the animal tissue procurement.

The costs of publication of this article were defrayed in part by the payment of page charges. This article must therefore be hereby marked *advertisement* in accordance with 18 U.S.C. Section 1734 solely to indicate this fact.

Received May 8, 2018; revised August 16, 2018; accepted September 11, 2018; published first September 28, 2018.

References

1. Im DS, Heise CE, Harding MA, George SR, O'Dowd BF, Theodorescu D, et al. Molecular cloning and characterization of a lysophosphatidic acid receptor, Edg-7, expressed in prostate. Mol Pharmacol 2000;57:753–9.
2. Ishii I, Contos JJ, Fukushima N, Chun J. Functional comparisons of the lysophosphatidic acid receptors, LP(A1)/VZG-1/EDG-2, LP(A2)/EDG-4, and LP(A3)/EDG-7 in neuronal cell lines using a retrovirus expression system. Mol Pharmacol 2000;58:895–902.
3. Jia W, Tran SK, Ruddick CA, Murph MM. The Src homology 3 binding domain is required for lysophosphatidic acid 3 receptor-mediated cellular viability in melanoma cells. Cancer Lett 2015;356:589–96.
4. Altman MK, Gopal V, Jia W, Yu S, Hall H, Mills GB, et al. Targeting melanoma growth and viability reveals dualistic functionality of the phosphonothionate analogue of carba cyclic phosphatidic acid. Mol Cancer 2010;9:140.
5. Yu S, Murph MM, Lu Y, Liu S, Hall HS, Liu J, et al. Lysophosphatidic acid receptors determine tumorigenicity and aggressiveness of ovarian cancer cells. J Natl Cancer Inst 2008;100:1630–42.
6. Liu S, Murph M, Panupinthu N, Mills GB. ATX-LPA receptor axis in inflammation and cancer. Cell Cycle 2009;8:3695–701.
7. Dvinge H, Git A, Graf S, Salmon-Divon M, Curtis C, Sottoriva A, et al. The shaping and functional consequences of the microRNA landscape in breast cancer. Nature 2013;497:378-82.
8. Harding C, Heuser J, Stahl P. Endocytosis and intracellular processing of transferrin and colloidal gold-transferrin in rat reticulocytes: demonstration of a pathway for receptor shedding. Eur J Cell Biol 1984;35:256–63.
9. Pan BT, Teng K, Wu C, Adam M, Johnstone RM. Electron microscopic evidence for externalization of the transferrin receptor in vesicular form in sheep reticulocytes. J Cell Biol 1985;101:942–8.
10. Subra C, Grand D, Laulagnier K, Stella A, Lambeau G, Paillasse M, et al. Exosomes account for vesicle-mediated transcellular transport of activatable phospholipases and prostaglandins. J Lipid Res 2010;51:2105–20.
11. Zaborowski MP, Balaj L, Breakefield XO, Lai CP. Extracellular vesicles: composition, biological relevance, and methods of study. Bioscience 2015;65:783–97.
12. Jethwa SA, Leah EJ, Zhang Q, Bright NA, Oxley D, Bootman MD, et al. Exosomes bind autotaxin and act as a physiological delivery mechanism to stimulate LPA receptor signalling in cells. J Cell Sci 2016;129:3948–57.
13. Peinado H, Aleckovic M, Lavotshkin S, Matei I, Costa-Silva B, Moreno-Bueno G, et al. Melanoma exosomes educate bone marrow progenitor cells toward a pro-metastatic phenotype through MET. Nat Med 2012;18:883–91.
14. Baj-Krzyworzeka M, Szatanek R, Weglarczyk K, Baran J, Urbanowicz B, Branski P, et al. Tumour-derived microvesicles carry several surface determinants and mRNA of tumour cells and transfer some of these determinants to monocytes. Cancer Immunol Immunother 2006;55:808–18.
15. Baj-Krzyworzeka M, Szatanek R, Weglarczyk K, Baran J, Zembala M. Tumour-derived microvesicles modulate biological activity of human monocytes. Immunol Lett 2007;113:76–82.
16. Valadi H, Ekstrom K, Bossios A, Sjostrand M, Lee JJ, Lotvall JO. Exosome-mediated transfer of mRNAs and microRNAs is a novel mechanism of genetic exchange between cells. Nat Cell Biol 2007;9:654–9.
17. Huber V, Filipazzi P, Iero M, Fais S, Rivoltini L. More insights into the immunosuppressive potential of tumor exosomes. J Transl Med 2008;6:63.
18. Iero M, Valenti R, Huber V, Filipazzi P, Parmiani G, Fais S, et al. Tumour-released exosomes and their implications in cancer immunity. Cell Death Differ 2008;15:80–8.
19. Isola AL, Chen S. Exosomes: the link between GPCR activation and metastatic potential? Front Genet 2016;7:56.
20. Margue C, Reinsbach S, Philippidou D, Beaume N, Walters C, Schneider JG, et al. Comparison of a healthy miRNome with melanoma patient miRNomes: are microRNAs suitable serum biomarkers for cancer? Oncotarget 2015;6:12110–27.
21. Wang G, Zhao Y, Zheng Y. MiR-122/Wnt/beta-catenin regulatory circuitry sustains glioma progression. Tumour Biol 2014;35:8565–72.
22. Xu J, Zhu X, Wu L, Yang R, Yang Z, Wang Q, et al. MicroRNA-122 suppresses cell proliferation and induces cell apoptosis in hepatocellular carcinoma by directly targeting Wnt/Beta-catenin pathway. Liver Int 2012;752–60.
23. Lai SL, Yao WL, Tsao KC, Houben AJ, Albers HM, Ovaa H, et al. Autotaxin/Lpar3 signaling regulates Kupffer's vesicle formation and left-right asymmetry in zebrafish. Development 2012;139:4439–48.
24. Alberts B, Johnson A, Lewis J, Morgan D, Raff M, Roberts K, et al. Molecular biology of the cell 6th edition. New York, NY: Garland Science; 2014.
25. Fang X, Yu S, Tanyi JL, Lu Y, Woodgett JR, Mills GB. Convergence of multiple signaling cascades at glycogen synthase kinase 3: Edg receptor-mediated phosphorylation and inactivation by lysophosphatidic acid through a protein kinase C-dependent intracellular pathway. Mol Cell Biol 2002;22:2099–110.
26. Jia W, Eneh JO, Ratnaparkhe S, Altman MK, Murph MM. MicroRNA-30c-2* expressed in ovarian cancer cells suppresses growth factor-induced cellular proliferation and downregulates the oncogene BCL9. Mol Cancer Res 2011;9:1732–45.
27. Hennessy BT, Lu Y, Gonzalez-Angulo AM, Carey MS, Myhre S, Ju Z, et al. A technical assessment of the utility of reverse phase protein arrays for the study of the functional proteome in non-microdissected human breast cancers. Clin Proteomics 2010;6:129–51.
28. Zhang L, Wei Q, Mao L, Liu W, Mills GB, Coombes K. Serial dilution curve: a new method for analysis of reverse phase protein array data. Bioinformatics 2009;25:650–4.
29. Hasegawa Y, Erickson JR, Goddard GJ, Yu S, Liu S, Cheng KW, et al. Identification of a phosphothionate analogue of lysophosphatidic acid (LPA) as a selective agonist of the LPA3 receptor. J Biol Chem 2003;278:11962–9.
30. Wu G, He X. Threonine 41 in beta-catenin serves as a key phosphorylation relay residue in beta-catenin degradation. Biochemistry 2006;45:5319–23.
31. Liang H, Ward WF. PGC-1alpha: a key regulator of energy metabolism. Adv Physiol Educ 2006;30:145–51.

32. Tan Z, Luo X, Xiao L, Tang M, Bode AM, Dong Z, et al. The role of PGC1alpha in cancer metabolism and its therapeutic implications. Mol Cancer Ther 2016;15:774–82.
33. Lanford RE, Hildebrandt-Eriksen ES, Petri A, Persson R, Lindow M, Munk ME, et al. Therapeutic silencing of microRNA-122 in primates with chronic hepatitis C virus infection. Science 2010;327:198–201.
34. Janssen HL, Reesink HW, Lawitz EJ, Zeuzem S, Rodriguez-Torres M, Patel K, et al. Treatment of HCV infection by targeting microRNA. N Engl J Med 2013;368:1685–94.
35. Iliopoulos D, Drosatos K, Hiyama Y, Goldberg IJ, Zannis VI. MicroRNA-370 controls the expression of microRNA-122 and Cpt1alpha and affects lipid metabolism. J Lipid Res 2010;51:1513–23.
36. Wu X, Somlo G, Yu Y, Palomares MR, Li AX, Zhou W, et al. De novo sequencing of circulating miRNAs identifies novel markers predicting clinical outcome of locally advanced breast cancer. J Transl Med 2012;10:42.
37. Fornari F, Gramantieri L, Giovannini C, Veronese A, Ferracin M, Sabbioni S, et al. MiR-122/cyclin G1 interaction modulates p53 activity and affects doxorubicin sensitivity of human hepatocarcinoma cells. Cancer Res 2009;69:5761–7.
38. Liu AM, Xu Z, Shek FH, Wong KF, Lee NP, Poon RT, et al. miR-122 targets pyruvate kinase M2 and affects metabolism of hepatocellular carcinoma. PLoS One 2014;9:e86872.
39. Mukherjee A, Ma Y, Yuan F, Gong Y, Fang Z, Mohamed EM, et al. Lysophosphatidic acid up-regulates hexokinase II and glycolysis to promote proliferation of ovarian cancer cells. Neoplasia 2015;17:723–34.
40. Fong MY, Zhou W, Liu L, Alontaga AY, Chandra M, Ashby J, et al. Breast-cancer-secreted miR-122 reprograms glucose metabolism in premetastatic niche to promote metastasis. Nat Cell Biol 2015;17:183–94.
41. Contos JJ, Chun J. The mouse lp(A3)/Edg7 lysophosphatidic acid receptor gene: genomic structure, chromosomal localization, and expression pattern. Gene 2001;267:243–53.

AACR American Association for Cancer Research

Molecular Cancer Research

miR-122-5p Expression and Secretion in Melanoma Cells Is Amplified by the LPAR3 SH3–Binding Domain to Regulate Wnt1

Charnel C. Byrnes, Wei Jia, Ali A. Alshamrani, et al.

Mol Cancer Res 2019;17:299-309. Published OnlineFirst September 28, 2018.